Polarized pulse waves in random discrete scatterers

Akira Ishimaru, Sermsak Jaruwatanadilok, and Yasuo Kuga

In recent years there has been increasing interest in the use of polarization for imaging objects in a cluttered environment. Examples are optical imaging through clouds, optical detection of objects in a biological medium, and microwave detection of objects in clutter. We extend previous studies of continuous-wave scattering to pulse-polarization scattering in discrete scatterers. We solve the time-dependent vector radiative transfer equation for a plane-parallel medium by using Mie scattering and the discrete ordinates method. The time-dependent degree of polarization and cross-polarization discrimination are calculated and verify the advantages of circular over linear polarization in maintaining greater copolarized components rather than cross-polarized components. © 2001 Optical Society of America

OCIS codes: 030.5620, 110.7050, 290.5850, 290.4020, 290.4210.

1. Introduction

There has been increasing interest in the use of polarization in imaging through cluttered media. Optical imaging through clouds and fog, imaging in biological media, and microwave detection in clutter can benefit from the additional information provided by the polarization characteristics. In particular, it was noted that circular polarization maintains its copolarized components farther into the medium than do cross-polarized components, thus helping to improve resolution.[1–7] Polarization pulse propagation in random media has also received attention; most of those studies were based on Monte Carlo calculations.[4–7] We previously conducted studies of cw polarized waves in discrete scatterers based on vector radiative transfer and the discrete ordinates method.[8–10] In this paper we extend our previous study to polarized pulses, based on time-dependent vector radiative transfer for a plane-parallel medium. We solve this time-dependent vector radiative transfer equation numerically, using the discrete ordinates method, by first modifying the radiative transfer equation to obtain an equation that is numerically stable. The Mueller matrix, including the size distributions, is obtained from Mie scattering. The solution in the frequency domain is then Fourier transformed to yield the pulse solution.

In this paper we study the specific intensity in a slab of a random medium of discrete spherical scatterers. We consider the pulse wave's intensity and its polarization characteristics as the optical depth varies. We analyze the time-resolved solutions when linear and circular polarized pulses are incident upon the random medium.

Numerical solutions are presented for latex spheres in water and for fog particles in air. The vector radiative transfer equation is solved by use of Mie scattering and the discrete ordinates method. Time-dependent Stokes vectors are obtained for linear and circular polarization waves in discrete scatterers. Specific intensities, degree of polarization, and cross-polarization discrimination are calculated as functions of optical depth and normalized time, verifying our conclusions regarding linear versus circular polarization. Also included are some discussions of time-dependent snake waves.

2. Modified Pulse Vector Radiative Transfer Equation

Consider narrow-band, time-dependent vector radiative transfer equations in a plane-parallel medium over optical distance domain τ, defined by $\tau = \rho\sigma_t z$, where ρ is the number density, σ_t is the total cross section of a single particle, and z is the actual distance in the medium measured from the incident side of the slab (Fig. 1). Note that τ_0 is the optical depth, defined by $\tau_0 = \rho\sigma_t L$, where L is length of the slab of

The authors are with the Department of Electrical Engineering, University of Washington, P.O. Box 352500, Seattle, Washington 98195-2500. The e-mail address for A. Ishimaru is ishimaru@ee.washington.edu.

Received 12 February 2001; revised manuscript received 21 May 2001.

0003-6935/01/305495-08$15.00/0

the random medium. The time-dependent vector radiative transfer equation is

$$\mu \frac{\partial}{\partial \tau}[\mathbf{I}(t, \tau, \mu, \phi)] + \left(1 + \frac{1}{\tau_0}\frac{\partial}{\partial t}\right)[\mathbf{I}(t, \tau, \mu, \phi)] = \int_0^{2\pi}\int_{-1}^{1} \mathbf{S}(\mu, \phi, \mu', \phi')][\mathbf{I}(t, \tau, \mu', \phi')]d\mu' d\phi' + \mathbf{F}_0(\mu, \phi) f(t, \tau), \qquad 0 \le \tau \le \tau_0, \quad (1)$$

where $\mathbf{I}$ is the modified Stokes parameter, defined by

$$\mathbf{I} = [I_1\ I_2\ U\ V]^{\mathrm{T}} = [\langle E_1 E_1^* \rangle \langle E_2 E_2^* \rangle 2\ \mathrm{Re}\langle E_1 E_2^* \rangle 2\ \mathrm{Im}\langle E_1 E_2^* \rangle]^{\mathrm{T}}, \quad (2)$$

where E_1 and E_2 are the electric field components in the θ and ϕ directions, respectively. An asterisk indicates a complex conjugate. Angle brackets mean an ensemble average. T denotes the transpose of a matrix. The boundary conditions of $\mathbf{I}$ are

$$\mathbf{I}(\tau = 0) = 0 \qquad 0 \le \mu \le 1,$$
$$\mathbf{I}(\tau = \tau_0) = 0 \qquad -1 \le \mu \le 0, \quad (3)$$

meaning that there is no other intensity coming into the slab of the random medium except input intensity. $\mu = \cos\theta$ is the cosine of the polar angle, $\mathbf{F}_0$ is the source term that corresponds to the incident flux magnitude, and $\mathbf{S}$ is the Mueller matrix defined in Eq. (10) below. t is the normalized time [actual time/(L/c)], where c is the speed of light in the medium. $f(t, \tau)$ is the input pulse at t and τ. If the input is a delta function, we have

$$f(t, \tau) = \exp(-\tau)\delta[t - (\tau/\tau_0)]. \quad (4)$$

If it is a Gaussian pulse, we have

$$f(t, \tau) = \frac{1}{\sqrt{\pi}\, T_0} \exp\left[-\tau - \frac{(t - \tau/\tau_0)^2}{T_0^2}\right], \quad (5)$$

where T_0 is the pulse duration.

Now we take the Fourier transform of Eq. (1) and obtain

$$\mu \frac{\partial}{\partial \tau}[\mathbf{I}(\omega, \tau, \mu, \phi)] + \left(1 - i\frac{\omega}{\tau_0}\right)[\mathbf{I}(\omega, \tau, \mu, \phi)] = \int_0^{2\pi}\int_{-1}^{1} \mathbf{S}(\mu, \phi, \mu', \phi')][\mathbf{I}(\omega, \tau, \mu', \phi')]d\mu' d\phi' + \mathbf{F}_0(\tau, \mu, \phi) f(\omega, \tau), \qquad 0 \le \tau \le \tau_0, \quad (6)$$

where

$$I(\omega, \tau, \mu, \phi) = \int I(t, \tau, \mu, \phi)\exp(i\omega t)dt \quad (7)$$

and $f(\omega, \tau)$ is given by

$$f(\omega, \tau) = \exp\left[-\left(1 - i\frac{\omega}{\tau_0}\right)\tau\right] \quad (8)$$

for a delta function input and by

$$f(\omega, \tau) = \exp\left(-\frac{\omega^2 T_0^2}{4}\right)\exp\left[-\left(1 - i\frac{\omega}{\tau_0}\right)\tau\right] \quad (9)$$

for a Gaussian pulse.

Note that Eq. (9) is identical to Eq. (8), except that it is multiplied by the Gaussian spectrum $\exp[-(\omega^2 T_0^2/4)]$. Mueller matrix $\mathbf{S}$ is given by[8]

$$\mathbf{S}(\mu, \phi, \mu', \phi') = \sigma_{t'} \begin{bmatrix} |f_{11}|^2 & |f_{12}|^2 & \mathrm{Re}(f_{11}f_{12}^*) & -\mathrm{Im}(f_{11}f_{12}^*) \\ |f_{21}|^2 & |f_{22}|^2 & \mathrm{Re}(f_{21}f_{22}^*) & -\mathrm{Im}(f_{21}f_{22}^*) \\ 2\ \mathrm{Re}(f_{11}f_{21}^*) & 2\ \mathrm{Re}(f_{12}f_{22}^*) & \mathrm{Re}(f_{11}f_{12}^* + f_{12}f_{21}^*) & -\mathrm{Im}(f_{11}f_{12}^* - f_{12}f_{21}^*) \\ 2\ \mathrm{Im}(f_{11}f_{21}^*) & 2\ \mathrm{Im}(f_{12}f_{22}^*) & \mathrm{Im}(f_{11}f_{22}^* + f_{12}f_{21}^*) & \mathrm{Re}(f_{11}f_{22}^* - f_{12}f_{21}^*) \end{bmatrix}, \quad (10)$$

where the scattering amplitudes f_{11}, f_{12}, f_{21}, and f_{22} are calculated by Mie theory, as explained in Appendix A.[9,10] For the development of the solution later in this paper, we write the Mueller matrix as

$$\mathbf{S} = \begin{bmatrix} \mathbf{S}_1 & \mathbf{S}_3 \\ \mathbf{S}_2 & \mathbf{S}_4 \end{bmatrix}. \quad (11)$$

In solving Eq. (6) numerically it will soon become apparent that the solution is highly unstable because of the presence of the high-frequency component $\exp(i\omega\tau/\tau_0)$ in Eq. (8) or (9). To obtain a stable solution we let

$$I(\omega, \tau) = I_d(\omega, \tau)\exp\left(i\frac{\omega}{\tau_0}\tau\right) \quad (12)$$

and obtain the modified vector radiative transfer equation

$$\mu \frac{\partial}{\partial \tau}[\mathbf{I}_d(\omega, \tau, \mu, \phi)] + \left[1 + (\mu - 1)i\frac{\omega}{\tau_0}\right] \times [\mathbf{I}_d(\omega, \tau, \mu, \phi)] = \int_0^{2\pi}\int_{-1}^{1} \mathbf{S}(\mu, \phi, \mu', \phi')][\mathbf{I}_d(\omega, \tau, \mu', \phi')]d\mu' d\phi' + \mathbf{F}_0(\tau, \mu, \phi) f_d(\omega, \tau), \qquad 0 \le \tau \le \tau_0, \quad (13)$$

where

$$f_d(\omega, \tau) = \begin{cases} \exp(-\tau) & \text{delta function pulse} \\ \exp(-\tau)\exp\left(-\dfrac{\omega^2 T_0^2}{4}\right) & \text{Gaussian pulse} \end{cases}. \quad (14)$$

The solution of Eq. (13) is in the frequency domain. To get the time-domain solution we use the Fourier transform given by

$$[\mathbf{I}_d(t, \tau)] = \frac{1}{2\pi}\int [\mathbf{I}_d(\omega, \tau)]\exp\left(i\frac{\omega}{\tau_0}\tau - i\omega t\right)\mathrm{d}\omega, \quad (15)$$

where $\mathbf{I}_d(t, \tau)$ is the diffuse Stokes vector in the time domain,

$$\mathbf{I}_d(t, \tau) = [I_1(t, \tau)\ I_2(t, \tau)\ U(t, \tau)\ V(t, \tau)]^{\mathrm{T}}. \quad (16)$$

3. Incidence of Linear Polarization

For a linearly polarized incident wave, the reduced (coherent) Stokes vector $\mathbf{I}_{ri}$ is

$$\mathbf{I}_{ri}(t, \tau) = [1\ 0\ 0\ 0]^{\mathrm{T}}\exp(-\tau). \quad (17)$$

The diffused specific intensity $\mathbf{I}_d(t, \tau)$ can be decomposed by use of the Fourier expansion as

$$\mathbf{I}_d(t, \tau, \mu, \phi) = \mathbf{I}_d^{(0)}(t, \tau, \mu) + \sum_{n=1}^{\infty}[\mathbf{I}_{dc}^{(n)}(t, \tau, \mu)\cos(n\phi) + \mathbf{I}_{ds}^{(n)}(t, \tau, \mu)\sin(n\phi)]. \quad (18)$$

For a normally incident plane wave, there are only two nonzero Fourier expansions, namely, mode zero ($n = 0$) and mode two ($n = 2$). They are also uncoupled. As a result, we can reduce radiative transfer equation (13) to two separate equations. The equation for mode zero is

$$\mu\frac{\partial}{\partial\tau}[\mathbf{I}_d^{(0)}(\omega, \tau, \mu)] + \left[1 + (\mu - 1)i\frac{\omega}{\tau_0}\right] \times [\mathbf{I}_d^{(0)}(\omega, \tau, \mu)] = \int_{-1}^{1}\mathbf{L}_1^{(0)}(\mu, \mu')][\mathbf{I}_d^{(0)}(\omega, \tau, \mu')]\mathrm{d}\mu' + \mathbf{F}_0^{(0)}(\mu)f_d(\omega, \tau),\ 0 \le \tau \le \tau_0, \quad (19)$$

where

$$\mathbf{I}_d^{(0)}(\tau, \mu) = \begin{bmatrix} I_1^{(0)}(\tau, \mu) \\ I_2^{(0)}(\tau, \mu) \end{bmatrix}, \quad (20)$$

$$\mathbf{F}_0^{(0)}(\mu) = \frac{1}{2\sigma_t}\begin{bmatrix} |A_{ll}(\mu)| \\ |A_{rr}(\mu)| \end{bmatrix},$$

$$\mathbf{L}_1^{(0)}(\mu, \mu') = \int_0^{2\pi}\mathbf{S}_1(\mu, \mu', \phi' - \phi)\mathrm{d}(\phi' - \phi). \quad (21)$$

$\mathbf{S}_1$ is from Eq. (11). The functions A_{ll} and A_{rr} are given in Appendix A.

In the same fashion, the equation for mode two is given by

$$\mu\frac{\partial}{\partial\tau}[\mathbf{I}_d^{(2)}(\omega, \tau, \mu)] + \left[1 + (\mu - 1)i\frac{\omega}{\tau_0}\right] \times [\mathbf{I}_d^{(2)}(\omega, \tau, \mu)] = \int_{-1}^{1}\mathbf{L}^{(2)}(\mu, \mu')][\mathbf{I}_d^{(2)}(\omega, \tau, \mu')]\mathrm{d}\mu' + \mathbf{F}_0^{(2)}(\mu)f_d(\omega, \tau), \quad 0 \le \tau \le \tau_0, \quad (22)$$

where

$$\mathbf{I}_d^{(2)}(\tau, \mu) = \begin{bmatrix} I_{1c}^{(2)}(\tau, \mu) \\ I_{1c}^{(2)}(\tau, \mu) \\ U_s^{(2)}(\tau, \mu) \\ V_s^{(2)}(\tau, \mu) \end{bmatrix},$$

$$\mathbf{F}_0^{(2)}(\mu) = \frac{1}{2\sigma_t}\begin{bmatrix} |A_{ll}(\mu)| \\ -|A_{rr}(\mu)| \\ -2\ \mathrm{Re}[A_{ll}(\mu)A_{rr}^*(\mu)] \\ -2\ \mathrm{Im}[A_{ll}(\mu)A_{rr}^*(\mu)] \end{bmatrix}, \quad (23)$$

$$\mathbf{L}^{(2)} = \begin{bmatrix} \mathbf{L}_1^{(2)} & \mathbf{L}_2^{(2)} \\ \mathbf{L}_3^{(2)} & \mathbf{L}_4^{(2)} \end{bmatrix}, \quad (24)$$

where

$$\mathbf{L}_1^{(2)}(\mu, \mu') = \int_0^{2\pi}\mathbf{S}_1(\mu, \mu', \phi' - \phi) \times \cos[2(\phi' - \phi)]\mathrm{d}(\phi' - \phi),$$

$$\mathbf{L}_2^{(2)}(\mu, \mu') = \int_0^{2\pi}\mathbf{S}_2(\mu, \mu', \phi' - \phi) \times \sin[2(\phi' - \phi)]\mathrm{d}(\phi' - \phi),$$

$$\mathbf{L}_3^{(2)}(\mu, \mu') = \int_0^{2\pi}\mathbf{S}_3(\mu, \mu', \phi' - \phi) \times \sin[2(\phi' - \phi)]\mathrm{d}(\phi' - \phi),$$

$$\mathbf{L}_4^{(2)}(\mu, \mu') = \int_0^{2\pi}\mathbf{S}_4(\mu, \mu', \phi' - \phi) \times \cos[2(\phi' - \phi)]\mathrm{d}(\phi' - \phi). \quad (25)$$

$\mathbf{S}_1$, $\mathbf{S}_2$, $\mathbf{S}_3$, and $\mathbf{S}_4$ are from Eq. (11).

Therefore the diffused Stokes intensity is the combination of the mode-zero diffused Stokes intensity

and the mode-two diffused Stokes intensity as follows:

$$\begin{aligned}\mathbf{I}_d(t, \tau, \mu, \phi) &= \mathbf{I}_d^{(0)}(t, \tau, \mu) + \mathbf{I}_{dc}^{(2)}(t, \tau, \mu)\cos(n\phi) \\ &\quad + \mathbf{I}_{ds}^{(2)}(t, \tau, \mu)\sin(n\phi) \\ &= \begin{bmatrix} I_1^{(0)}(t, \tau, \mu) \\ I_2^{(0)}(t, \tau, \mu) \\ 0 \\ 0 \end{bmatrix} \\ &\quad + \begin{bmatrix} I_{1c}^{(2)}(t, \tau, \mu)\cos(2\phi) \\ I_{2c}^{(2)}(t, \tau, \mu)\cos(2\phi) \\ U_s^{(2)}(t, \tau, \mu)\sin(2\phi) \\ V_s^{(2)}(t, \tau, \mu)\sin(2\phi) \end{bmatrix}. \end{aligned} \tag{26}$$

4. Incidence of Circular Polarization

For circularly polarized incidence, the reduced (coherent) Stokes vector $\mathbf{I}_{ri}$ is

$$\mathbf{I}_{ri}(t, \tau) = [1/2\ 1/2\ 0\ 1]^{\mathrm{T}} \exp(-\tau). \tag{27}$$

By the same Fourier series decomposition of the diffused Stokes intensity as in the linearly polarized case, the only nonzero mode is mode zero ($n = 0$). Also, the radiative transfer equation is uncoupled into two separate equations that can be solved independently:

$$\begin{aligned}\mu \frac{\partial}{\partial \tau}[\mathbf{I}_{d1}^{(0)}(\omega, \tau, \mu)] + \left[1 + (\mu - 1)i\frac{\omega}{\tau_0}\right] \\ \times [\mathbf{I}_{d1}^{(0)}(\omega, \tau, \mu)] \\ = \int_{-1}^{1} \mathbf{L}_1^{(0)}(\mu, \mu')][\mathbf{I}_{d1}^{(2)}(\omega, \tau, \mu')]\mathrm{d}\mu' \\ + \mathbf{F}_1^{(0)}(\mu) f_d(\omega, \tau), \qquad 0 \le \tau \le \tau_0, \end{aligned} \tag{28}$$

$$\begin{aligned}\mu \frac{\partial}{\partial \tau}[\mathbf{I}_{d2}^{(0)}(\omega, \tau, \mu)] + \left[1 + (\mu - 1)i\frac{\omega}{\tau_0}\right] \\ \times [\mathbf{I}_{d2}^{(0)}(\omega, \tau, \mu)] \\ = \int_{-1}^{1} \mathbf{L}_4^{(0)}(\mu, \mu')][\mathbf{I}_{d2}^{(2)}(\omega, \tau, \mu')]\mathrm{d}\mu' \\ + \mathbf{F}_2^{(0)}(\mu) f_d(\omega, \tau), \qquad 0 \le \tau \le \tau_0, \end{aligned} \tag{29}$$

where

$$\begin{aligned}\mathbf{I}_{d1}^{(0)}(\tau, \mu) &= \begin{bmatrix} I_1^{(0)}(\tau, \mu) \\ I_2^{(0)}(\tau, \mu) \end{bmatrix}, \\ \mathbf{F}_1^{(0)}(\mu) &= \frac{1}{2\sigma_t}\begin{bmatrix} |A_{ll}(\mu)| \\ |A_{rr}(\mu)| \end{bmatrix}, \end{aligned} \tag{30}$$

$$\begin{aligned}\mathbf{I}_{d2}^{(0)}(\tau, \mu) &= \begin{bmatrix} U^{(0)}(\tau, \mu) \\ V^{(0)}(\tau, \mu) \end{bmatrix}, \\ \mathbf{F}_2^{(0)}(\mu) &= \frac{1}{\sigma_t}\begin{bmatrix} -\mathrm{Im}[A_{ll}(\mu)A_{rr}{}^*(\mu)] \\ \mathrm{Re}[A_{ll}(\mu)A_{rr}{}^*(\mu)] \end{bmatrix}. \end{aligned} \tag{31}$$

Table 1. Particle-Size Distribution of Latex Spheres

Diameter (μm)	Number of Particles
1.984	1
2.000	1
2.002	7
2.005	3
2.007	6
2.012	1
2.013	1
2.021	3
2.022	5
2.023	7
2.031	5
2.033	10
2.036	1
2.039	1
2.043	1

The diffused specific Stokes intensity is

$$\begin{aligned}\mathbf{I}_d(t, \tau, \mu) &= \mathbf{I}_{d1}^{(0)}(t, \tau, \mu) + \mathbf{I}_{d2}^{(0)}(t, \tau, \mu) \\ &= [I_1^{(0)}(\tau, \mu)\ I_2^{(0)}(\tau, \mu)\ U^{(0)}(\tau, \mu) \\ &\quad \times V^{(0)}(\tau, \mu)]^{\mathrm{T}} \\ &\equiv [I_1\ I_2\ U_2\ V_2]^{\mathrm{T}}. \end{aligned} \tag{32}$$

The left-handed and right-handed circularly polarized intensities are given by

$$I_{\mathrm{lhc}} = (I_1 + I_2 + V)/2, \quad I_{\mathrm{rhc}} = (I_1 + I_2 - V)/2. \tag{33}$$

5. Numerical Solutions for Latex Microspheres Suspended in Water

We solved Eqs. (19) and (22) for linear polarization and Eqs. (28) and (39) for circular polarization by using the discrete ordinates method. Our calculations use 0.53-μm light in water. To study the effect of the size of the particle, we used particle diameters 0.22, 0.48, and 1.05 μm, corresponding to size parameters (ka) 1.23, 2.69, and 5.89, respectively. In other calculations we used the particle-size distribution listed in Table 1. We applied the Gauss quadrature to the μ domain, using a total of 40 points. Throughout the paper we are interested only in the forward ($\theta = 3°$, $\tau = \tau_0$), off-axis ($\theta = 40°$, $\tau = \tau_0$), and backward ($\theta = 180°$, $\tau = 0$) portions of the results. For continuous waves we solved these equations for only the zero frequency. We calculated the specific intensity and the degree of polarization as a function of optical depth. The degree of polarization is defined as

$$m = \frac{[(I_1 - I_2)^2 + U^2 + V^2]^{1/2}}{I_1 + I_2}. \tag{34}$$

The cross-polarization discrimination (XPD) shows the ratio of copolarized to cross-polarized components:

$$\mathrm{XPD} = 10\ \log\left[\frac{I_{\text{co-pol}}}{I_{x\text{-pol}}}\right]. \tag{35}$$

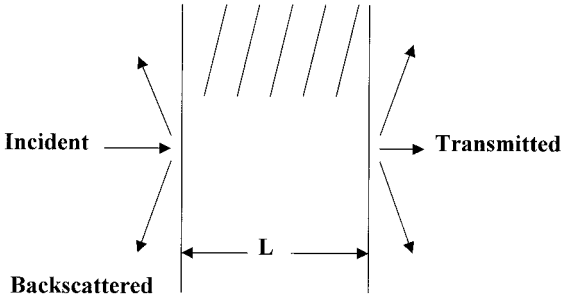

Fig. 1. The incident wave is a linearly or a circularly polarized wave. The medium comprises randomly distributed spherical scatterers.

For the pulse case, the input pulse is the Gaussian pulse with a width of 1/10 of the normalized time. The normalized time is defined by actual time divided by (L/c), where L is the length of the slab of the random medium and c is the speed of light in the medium.

In the pulse calculation we consider the number of frequencies used to resolve the time-dependent function. This involves stability of the solution and the computer resources available. These issues are not discussed here. We used 1001 frequency points with a total time length of 50 normalized time. The results that we got from solving Eqs. (19), (22), (28), and (29) are only diffused intensity with impulse input. As a result, the diffused intensity when the input pulse is Gaussian is the convolution of the input pulse with the time-resolved results in Eqs. (26) and (32). For linear polarization, the copolarized intensity is I_1 and the cross-polarized intensity is I_2. For circular polarization, the copolarized intensity is I_{lhc} and the cross-polarized intensity is I_{rhc}. In the forward direction, the total intensity is a combination of reduced intensity and diffused intensity, where θ is the field of view in radians:

$$I_{\mathrm{total}}(t) = I_{\mathrm{ri}} + (\pi\theta^2) I_d(t). \tag{36}$$

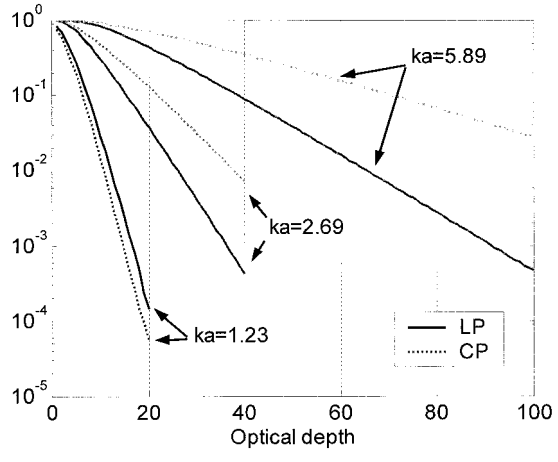

Fig. 2. Degree of polarization (in decibels) versus optical depth when size parameter (ka) varies.

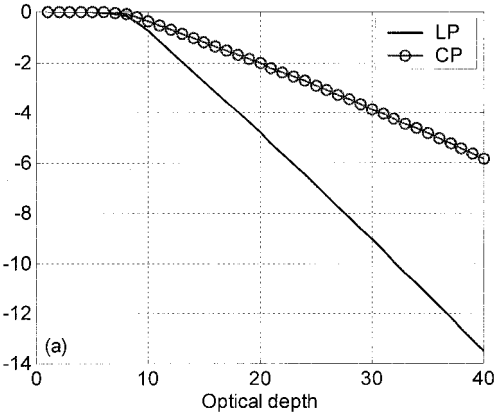

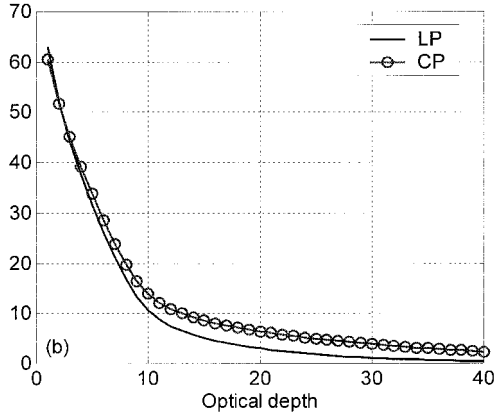

Fig. 3. (a) DOP and (b) XPD in the forward direction (in decibels) as a function of optical depth.

The total intensity is only the diffused intensity for the off-axis and backward directions, because the reduced intensity is zero in those cases. The results of the calculations are as follows:

A. Effects of Size on Degree of Polarization

The effects of size on the degree of polarization are shown in Fig. 2. For small size, the degree of polarization (DOP) is greater for linear polarization (LP) than for circular polarization (CP), whereas for large size, the degree of polarization for CP is greater than for LP.

B. DOP and XPD versus Optical Depth

Circular polarization maintains its DOP better than LP for both forward (Fig. 3) and backward (Fig. 4) scattering. Generally, CP gives a higher XPD than LP. For backward scattering, CP maintains its DOP better than LP. However, XPD is higher for LP than for CP.

C. Snake Waves in the Near-Forward Direction

Snake waves for CP are greater than for LP in small optical depth, as shown in Fig. 5.

D. Pulsed Scattered Waves in Forward and Backward Directions

Pulsed scattered waves exhibit the characteristic that CP is generally superior to LP in terms of DOP

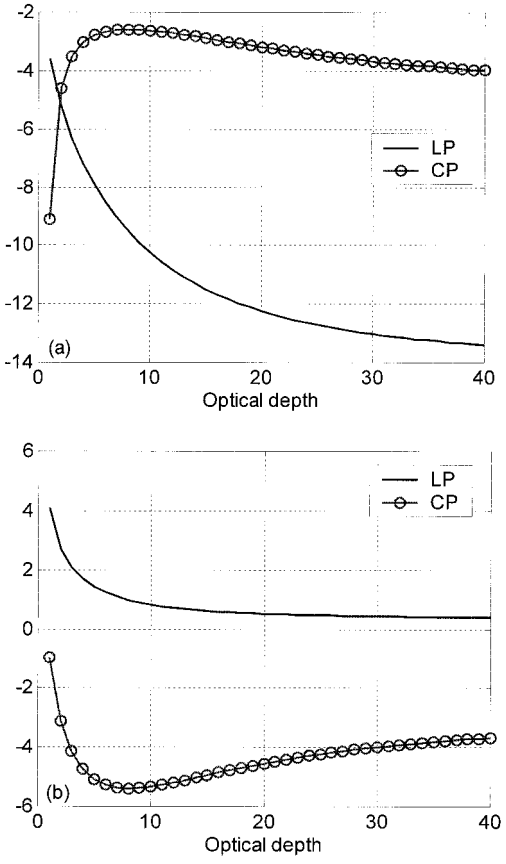

Fig. 4. (a) DOP and (b) XPD in the backward direction (in decibels) as a function of optical depth.

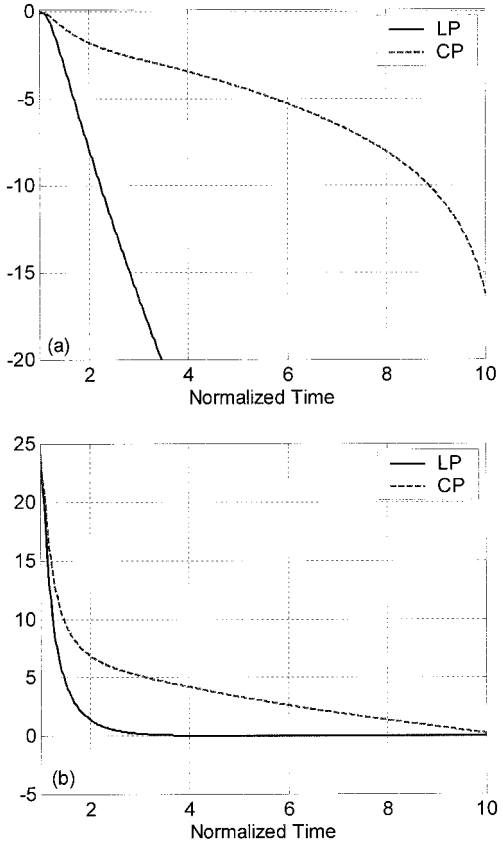

Fig. 6. (a) DOP and (b) XPD of the forward direction (in decibels) as a function of time ($\tau_0 = 10$).

and XPD for forward scattering, as shown in Fig. 6. However, in the backward direction, the XPD for LP is higher, as illustrated in Fig. 7. We use $\tau_0 = 10$ in both cases.

E. Pulsed Snake Waves

The strong presence of snake waves is apparent for small optical depths for the results compared in Fig. 8. Figure 8(a) shows the pulsed snake wave in for $\tau_0 = 1$, which exhibits greater intensity than that for $\tau_0 = 10$ shown in Fig. 8(b).

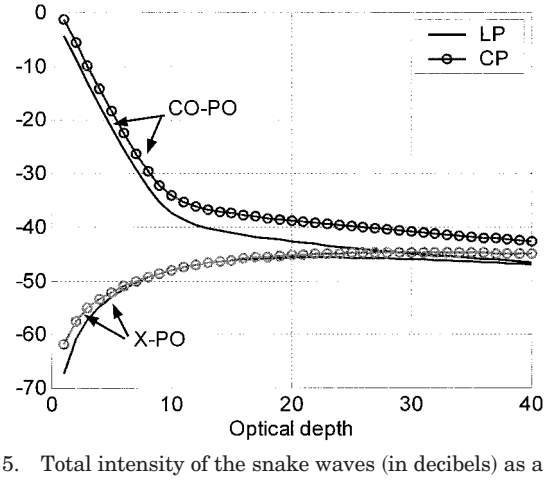

Fig. 5. Total intensity of the snake waves (in decibels) as a function of optical depth. CO-PO, copolarized; X-PO, cross polarized.

6. Numerical Solutions for Pulse Scattering in Fog Particles

We use a wavelength of 1 μm over a distance of 1 km, giving an optical depth of 1.16. The diameters of the fog particles are listed in Table 2. The results are summarized as follows:

A. DOP and XPD As Functions of Normalized Time

Figures 9 and 10 show the DOP and the XPD for $\lambda = 1$ μm in the forward and backward directions, respectively. Results indicate that, as time increases, CP maintains its degree of polarization better than LP in the forward and off-axis directions.

B. Pulsed Snake Waves

Pulsed snake waves for $\lambda = 1$ μm are shown in Fig. 11. The presence of snake waves is evident.

Table 2. Particle-Size Distribution of Fog

	Diameter of Particle (μm)							
Distribution	0.4	0.6	0.7	1.4	2	3.6	5.4	8
Number of particles	3	10	40	50	7	1	9	2

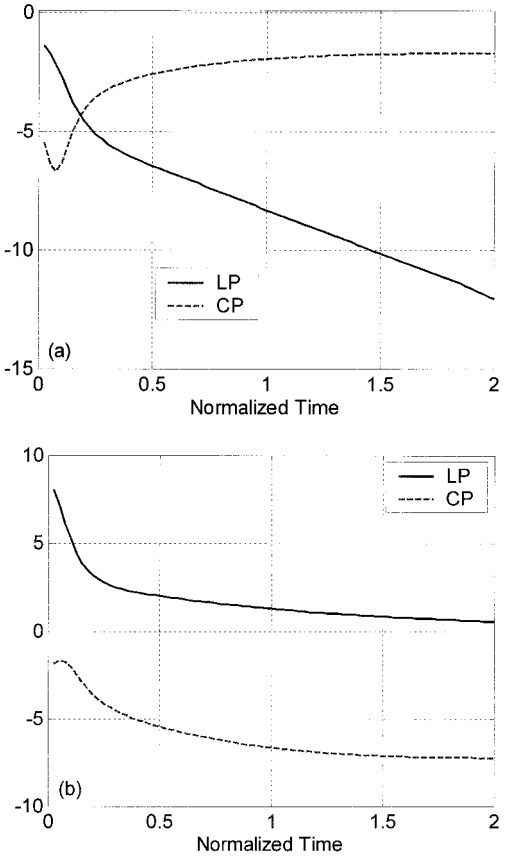

Fig. 7. (a) DOP and (b) XPD of the backward direction (in decibels) as a function of time ($\tau_0 = 10$).

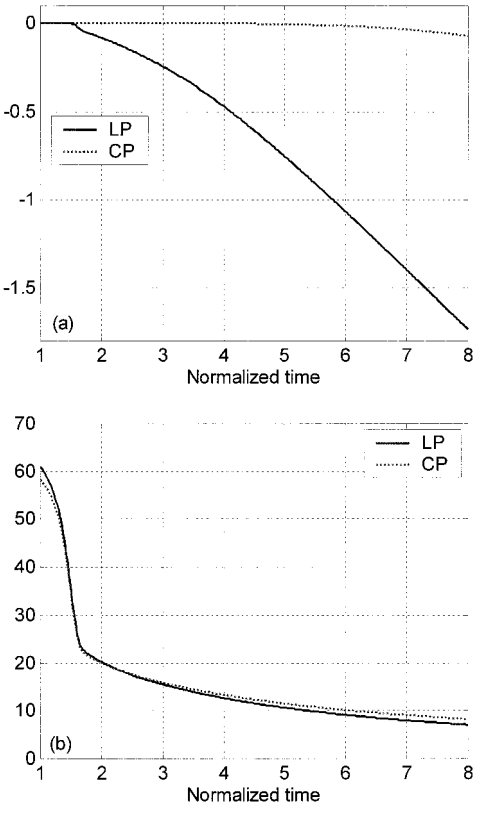

Fig. 9. (a) DOP and (b) XPD of the forward direction (in decibels) as a function of time (fog, $\lambda = 1$ μm).

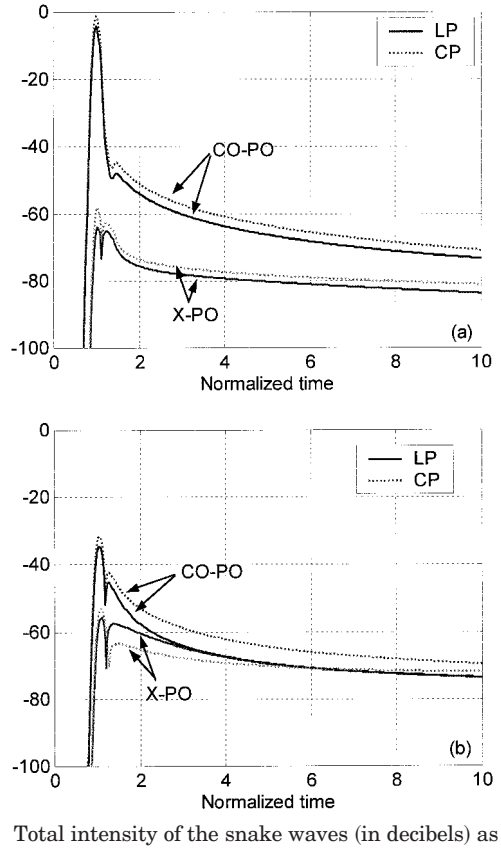

Fig. 8. Total intensity of the snake waves (in decibels) as a function of time: (a) $\tau_0 = 1$ and (b) $\tau_0 = 10$.

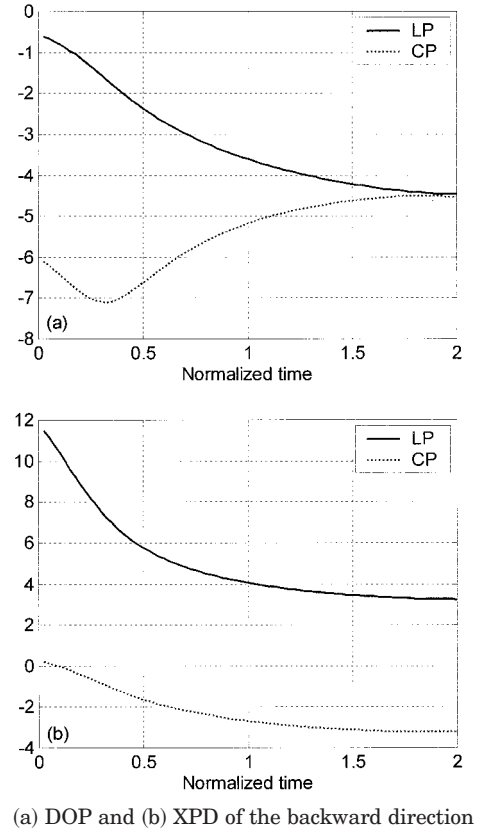

Fig. 10. (a) DOP and (b) XPD of the backward direction (in decibels) as a function of time (fog, $\lambda = 1$ μm).

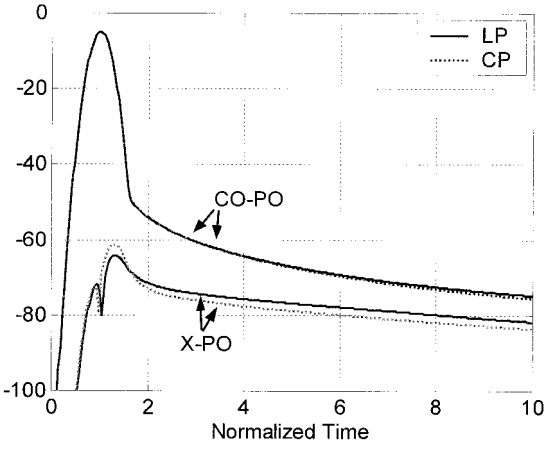

Fig. 11. Total intensity of the snake waves (in decibels) as a function of time (fog, $\lambda = 1\ \mu m$).

7. Conclusions

We have developed a numerically stable, modified vector radiative transfer formulation for polarized pulse scattering in random media. The solution for this vector radiative transfer equation is used to show the difference between circular and linear polarization and near-axis and off-axis scattering. In general, circular polarization has higher copolarized and lower cross-polarized components than linear polarization, and these characteristics may be used to improve imaging in a cluttered environment. It is also shown that the near-axis intensities are considerably higher than the off-axis intensities, indicating the snake wave phenomenon.

Appendix A

For spherical particles it is convenient to express f_{ij} in the following notation[10,11]:

$$
\begin{aligned}
f_{11} &= (l, l)T_1 + (r, r)T_2, \\
f_{12} &= -(r, l)T_1 + (l, r)T_2, \\
f_{21} &= -(l, r)T_1 + (r, l)T_2, \\
f_{22} &= (r, r)T_1 + (l, l)T_2, \\
(l, l) &= [(1 - \mu^2)(1 - \mu'^2)]^{1/2} + \mu\mu' \cos(\phi' - \phi), \\
(l, r) &= -\mu' \sin(\phi' - \phi), \\
(r, l) &= \mu' \sin(\phi' - \phi), \\
(r, r) &= \cos(\phi' - \phi), \\
T_1(x) &= \frac{A_{rr}(\chi) - \chi A_{ll}(\chi)}{1 - \chi^2}, \\
T_2(x) &= \frac{A_{ll}(\chi) - \chi A_{rr}(\chi)}{1 - \chi^2}, \qquad \text{(A1)}
\end{aligned}
$$

where

$$
\begin{aligned}
\chi = \cos\Theta &= [(1 - \mu^2)(1 - \mu'^2)]^{1/2} \cos(\phi' - \phi) \\
&\quad + \mu\mu', \\
\mu = \cos\theta, &\quad \mu' = \cos\theta'. \qquad \text{(A2)}
\end{aligned}
$$

(θ, ϕ) and (θ', ϕ') correspond to the incident and scattered wave directions, respectively, and Θ is the angle between the incident and the scattered waves. A_{ll} and A_{rr} are functions of Θ, and they are related to the scattering functions s_1 and s_2, respectively, used by van de Hulst[12] for the Mie solution:

$$A_{ll} = is_2^*/k, \qquad A_{rr} = is_1^*/k. \qquad \text{(A3)}$$

Here the conjugates of s_1 and s_2 are taken because van de Hulst used $\exp(j\omega t)$ dependence, whereas in this paper we use $\exp(-i\omega t)$ dependence.

This study is supported by the National Science Foundation (grant ECS-9908849), the U.S. Office of Naval Research (grant N000140010027), and the U.S. Air Force Research Laboratory (grant F29601-00-C-0240). We thank Arnold D. Kim for his early research on pulse vector radiative transfer. We also thank Charles Matson, U.S. Air Force Research Laboratory, for many discussions, comments, and suggestions.

References

1. D. Bicout, C. Brosseau, A. S. Martinez, and J. M. Schmitt, "Depolarization of multiply scattered waves by spherical diffusers: influence of the size parameter," Phys. Rev. E **49,** 1767–1770 (1994).
2. S. G. Demos and R. R. Alfano, "Optical polarization imaging," Appl. Opt. **36,** 150–155 (1997).
3. K. M. Yoo and R. R. Alfano, "Time resolved depolarization of multiple backscattered light from random media," Phys. Lett. A **142,** 531–536 (1989).
4. G. D. Lewis, D. L. Jordan, and P. J. Roberts, "Backscattering target detection in a turbid medium by polarization discrimination," Appl. Opt. **38,** 3937–3944 (1999).
5. M. Moscoso, J. B. Keller, and G. C. Papanicolaou, "Depolarization and blurring of optical images by biological tissue," J. Opt. Soc. Am. A **18,** 948–960 (2001).
6. A. D. Kim, S. Jaruwatanadilok, A. Ishimaru, and Y. Kuga, "Polarized light propagation and scattering in random media," in *Laser–Tissue Interaction XII: Photochemical, Photothermal, and Photomechanical*, D. D. Duncan, S. L. Jacques, and P. C. Johnson, eds., Proc. SPIE **4257,** 90–100 (2001).
7. P. Bruscaglioni, G. Zaccanti, and Q. Wei, "Transmission of a pulsed polarized light beam through thick turbid media: numerical results," Appl. Opt. **32,** 6142–6150 (1993).
8. A. Ishimaru, *Wave Propagation and Scattering in Random Media* (Institute of Electrical and Electronics Engineers, New York, 1997).
9. A. Ishimaru and R. L.-T. Cheung, "Multiple scattering effects on wave propagation due to rain," Ann. Telecommun. **35,** 373–379 (1980).
10. R. L.-T. Cheung and A. Ishimaru, "Transmission backscattering and depolarization of waves in randomly distributed spherical particles," Appl. Opt. **21,** 3792–3798 (1982).
11. Z. Sekera, "Scattering matrices and reciprocity relationships for various representations of the state of polarization," J. Opt. Soc. Am. **56,** 1732–1740 (1966).
12. H. C. van de Hulst, *Light Scattering by Small Particles* (Wiley, New York, 1957).